Ind. J. Pharm. Edu. Res., 2027; 61:10.5530/ijper.20270039.
https://www.ijper.org

Original Article

Development and Optimization of Dapsone-Loaded Transferosomal Gel for Enhanced Topical Delivery in *Acne vulgaris* Using a Box-Behnken Design

Venkatesh Aditiyaa Narayanaa*, Vanitha Sureshkumar*, Priya Palanisamy, Sambathkumar Ramanadhan

Department of Pharmaceutics, The Erode College of Pharmacy, The Tamil Nadu Dr. M.G.R. Medical University, Erode, Tamil Nadu, INDIA.

ABSTRACT

Objectives: The objective of this study was to develop, optimize, and evaluate a dapsone-loaded transferosomal gel for enhanced topical delivery in acne vulgaris using a Box-Behnken Design (BBD). *Acne vulgaris* is an inflammation-based dermatological condition that demands efficient treatment at the site of application. While dapsone is known for its antibacterial and anti-inflammatory actions, low aqueous solubility and lack of skin permeation are among the factors that restrict its pharmacological activity. The use of transferosomal nano-vesicles offers deformability and increased permeability. **Materials and Methods:** The development of transferosomes was performed using a three factors-three levels Box-Behnken design, which involved soya lecithin, Span 80, and chloroform methanol solvents. Vesicle size, entrapment efficiency, zeta potential, and drug release were used as response variables. Optimization was used to produce an optimized formula that was further loaded into a Carbopol 940 gel and characterized using FTIR, SEM, physiochemical parameters, *in vitro* drug release, drug release kinetics, antioxidant activity, antibacterial activity, and stability studies. **Results:** The optimal transferosomal gel possessed nanovesicles with high entrapment efficiency, Desirable zeta potential, and sustained drug release behaviour as per Korsmeyer-Peppas equation with a non-Fickian diffusion mechanism. The formulation showed excellent physicochemical characteristics, remarkable stability, strong antioxidant behaviour, and improved antibacterial action against *Staphylococcus aureus* and *Escherichia coli*. **Conclusion:** The optimized dapsone-loaded transferosomal gel represents a promising nanovesicular system for improved topical management of acne vulgaris through enhanced drug delivery and sustained therapeutic performance.

Keywords: Acne vulgaris, Box-Behnken design, Dapsone, Entrapment efficiency, Nanovesicular drug delivery, Quality by Design, Sustained drug release, Topical drug delivery, Transferosomal gel, Transferosomes.

Correspondence:
Mrs. Vanitha Sureshkumar
Department of Pharmaceutics, The Erode College of Pharmacy, The Tamil Nadu Dr. M.G.R. Medical University, Erode, Tamil Nadu, INDIA.
Email: vanithaecp2021@gmail.com

Venkatesh Aditiyaa Narayanaa
Department of Pharmaceutics, The Erode College of Pharmacy, The Tamil Nadu Dr. M.G.R. Medical University, Erode, Tamil Nadu, INDIA.
Email: anvenkatesh18@gmail.com

Received: 22-06-2026;
Revised: 11-08-2026;
Accepted: 02-09-2026.

INTRODUCTION

Acne vulgaris is one of the most prevalent chronic inflammatory disorders of the pilosebaceous unit, affecting approximately 80-90% of adolescents and a considerable proportion of adults.[1,2] The disease is characterized by comedones, papules, pustules, nodules, and inflammatory lesions resulting from follicular hyperkeratinization, excessive sebum production, proliferation of *Cutibacterium acnes*, and associated inflammatory responses.[2,3] Acne is strongly linked to significant psychological morbidity, including chronic disfigurement, scarring and public stigma which lead to decreased self-esteem, anxiety and depression, especially in adolescents and young adults, with a significant individual and socioeconomic burden and is a global phenomenon.[2,3]

Topical therapy is still the first line treatment for mild to moderate acne, as it is the most effective treatment which delivers the drug locally and produces the least systemic side effects.[4,5] Retinoids, benzoyl peroxide, antibiotics or a combination of more than one of these agents are used in conventional topical preparations currently in clinical use, such as gels, creams, and lotions.[4,5] However, these products have known drawbacks such as sensitivity, erythema, dryness, photosensitivity in the case of retinoids, resistance and disruption of the microbiome in the case of antibiotic monotherapy and contact sensitization in the case of benzoyl peroxide.[5] The outermost layer of the epidermis is called the stratum corneum, is composed of tightly packed corneocytes surrounded by an intercellular lipid matrix, is the single most important barrier that obstructs all conventional topical formulations. It represents a very strong physicochemical barrier and limits the passive diffusion of most therapeutic products,

DOI: 10.5530/ijper.20270039

Copyright Information :
Copyright Author (s) 2027 Distributed under Creative Commons CC-BY 4.0

Publishing Partner : Manuscript Technomedia. [www.mstechnomedia.com]

especially of polar molecules and products with poor partition coefficient, to obtain an appropriate concentration of the drugs in the pilosebaceous unit.[6-9]

Dapsone (4,4′-diaminodiphenyl sulfone) is a synthetic sulfone antimicrobial agent that has attracted a great deal of interest as a topical anti-acne agent for its dual mode of action.[9-11] It has direct antibacterial properties against *Cutibacterium acnes*, inhibiting dihydropteroate synthase in the folate synthesis pathway, and it also has anti-inflammatory properties, by inhibiting the production of pro-inflammatory mediators in the local inflammatory cascade.[9-11] Despite such therapeutically beneficial properties, conventional dapsone formulations suffer from poor aqueous solubility, sub-optimal trans-epidermal penetration, and insufficient retention of the drug in the deeper layers of the skin (dermis and pilosebaceous follicles) and consequently, the bioavailability of the drug in the area is low, and therapeutic performance is limited. Furthermore, dapsone can be oxidized leading to the difficulty of long-term stability of traditional dosage forms.[9,11,12] Consequently, the creation of an advanced delivery platform to optimize skin penetration, increase the amount of time a drug remains in the body, improve formulation stability, and prolong drug availability locally is an unmet therapeutic need.[11-13]

Transferosomes are a class of nanocarriers that have been found to be promising ultra-deformable lipid vesicles which can penetrate the barrier properties of the skin.[6-8,14] The vesicles are made of phospholipids and edge activators which allow the lipid bilayer to become elastic so that the vesicles can squeeze through narrow intercellular spaces in the Stratum Corneum cells.[7,17] The therapeutic efficiency of transferosomes is increased due to their peculiar deformability, which increases drug penetration, retains the drugs in the skin and gives sustained release properties as compared with systemic exposure.[12-16] Transferosomes are especially ideal for the topical delivery of poorly permeable drugs for dermatological applications due to these properties.[7,17,18]

Although transferosomal system has been widely studied for topical administration of different dermatological agents, only few reports have described the formulation of dapsone loaded transferosomal gel. transferosomal systems have been used for topical administration of various dermatological agents and dapsone has been widely used in conventional topical formulations for acne vulgaris.[10,14,15,17] The incorporation of dapsone into ultra-deformable transferosomal vesicles may result in better skin permeation, targeting to the follicles, and prolonged drug release which are some of the drawbacks of conventional formulations.[6-8,18] Thus, the present study was planned to prepare and optimize a transferosomal gel of dapsone for better topical treatment of acne vulgaris by applying Box-Behnken experimental design. The optimized formulation was further characterized for its physicochemical properties, vesicular morphology, entrapment efficiency, *in vitro* drug release, and stability. In addition, its antibacterial activity against *Staphylococcus aureus* and *Escherichia coli* was evaluated and compared with a marketed dapsone gel (Acnedap® gel) to assess its potential as an effective topical anti-acne formulation.

MATERIALS AND METHODS

Materials

Dapsone (4,4'-Diaminodiphenyl Sulfone (DDS)) was procured from Dhamtec Pharma and Consultants. Soya lecithin served as the phospholipid bilayer-forming agent, and Span 80 (sorbitan monooleate) was employed as the edge activator to confer membrane flexibility. Methanol and chloroform were used as the organic solvent phase, whereas distilled water served as the aqueous phase. Carbopol 940 was used as the gelling agent, with polyethylene glycol 400 (PEG 400) as humectant/plasticizer, Triethanolamine (TEA) as neutralizing agent, and methylparaben (0.1% w/w) as preservative. All chemicals and reagents chosen were analytical grade and purchased from Sigma-Aldrich.

Preformulation Studies

Determination of λ_{max}

A primary stock solution of dapsone at 1000 µg/mL concentration was in methanol and was diluted serially to obtain a working solution of 10 µg/mL concentration. The solution was scanned from 200 nm to 400 nm using a UV-visible Spectrophotometer Shimadzu UV-1900 UV-visible Spectrophotometer (Shimadzu Corporation, Kyoto, Japan) with methanol as a blank. The wavelength at which the solution gave maximum absorbance was taken as λ_{max}.[19]

Calibration Curve

A working stock solution (10 µg/mL) of dapsone was prepared in a phosphate buffer-methanol diluent (70:30 v/v). Aliquots were diluted to obtain final concentrations of 2, 4, 6, 8, and 10 µg/mL, and the absorbance of each standard was measured at λ_{max}=295 nm against diluent as blank to construct the calibration curve.[19,20]

Compatibility Study (FTIR)

FTIR spectra of dapsone, soya lecithin, Span 80, physical mixture, and the final gel formulation were recorded by the Attenuated Total Reflectance (ATR) method over the range 4000-400 cm^{-1}, following a background scan, to confirm drug identity and assess drug-excipient compatibility and the final formulation to assess chemical compatibility and detect interactions.[21-24]

Preparation of Dapsone Transferosomes by Solvent Injection Method

The soya lecithin and span 80 was first dissolved in chloroform to create the homogeneous lipid phase while dapsone was dissolved in methanol. The two phases were mixed to create the organic phase which was then filled in a syringe equipped with a 24-gauge

needle. Slow injection of one drop per 2 to 3 sec of the organic phase into pre-heated 50-55°C distilled water under magnetic stirring REMI Magnetic Stirrer (REMI Equipment, India) at 800-1000rpm, kept 4-5 cm above the aqueous surface leads to the formation of spontaneous self-assembly of phospholipid vesicles. The mixture is stirred for 30-35 min, rested for 1-2 hr followed by probe sonication in pulsed mode for 2-3 min at 25-30% amplitude at 40°C.[25]

Preparation of Transferosome-Loaded Gel

The Carbopol 940 (100 mg) was dissolved in distilled water (15 mL) and allowed to swell for 2-3 hr. Methylparaben (0.1% w/w), which was pre-dissolved in PEG 400, was added. Triethanolamine was added gradually in order to neutralize the mixture (pH 6.5-7.5). Ionization of polymers caused their expansion and formation of transparent gel base. The transferosome dispersion, which was optimized, was added drop by drop in the gel base with gentle circular stirring in order not to disrupt phospholipid bilayer. The overall preparation workflow is summarized schematically in Figure 1.

Experimental Design and Optimization

The formulation was optimized through a Quality by Design (QbD) process with Box-Behnken Design of experiment (BBD) consisting of three factors and three levels per factor using Design-Expert® 13 software. In order to optimize the formulation, three independent variables were identified through a set of initial trials. These were the concentration of lipid (phospholipid 90G/ soya lecithin; A, 100-200 mg), the concentration of edge activator (Span 80; B, 20-30 mg), and the ratio of chloroform to methanol as the solvent system (C, 1.2-1.8). The four dependent variables were vesicle size (R^1, minimum), encapsulation efficiency (R^2, maximum), zeta potential (R^3, absolute maximum), and *in vitro* drug release (R^4, maximum). Independent variable levels are summarized in Table 1.

Characterization of Transferosomes

Particle Size and Polydispersity Index

The particle size as well as Polydispersity Index (PDI) of the prepared transferosomes were measured by Dynamic Light Scattering (DLS) with a NanoPlus particle size analyzer (Particulate Systems, version 5.22/3.00). Samples were suitably diluted with water and analysed at 25°C. Measurements were performed in triplicate, and the mean particle size (nm) and PDI were recorded. Size distribution data were analysed using the Cumulants method and CONTIN algorithm.[26,27]

Zeta Potential

The zeta potential of the optimized transferosomal formulation was measured using a Zetasizer based on Electrophoretic Light Scattering (ELS). The formulation was diluted with distilled water to a suitable concentration for measurement prior to analysis. The conductivity of the diluted sample was measured and recorded as 0.1423 mS/cm before zeta potential analysis. The zeta potentials were then measured and the zeta potential value obtained used as an indicator of the colloidal stability of the formulation. The measurement was carried out at 25±1°C in a disposable folded capillary cell. The results were obtained and analysed in triplicates (n=3) and the pH of the diluted sample was kept at 7.0±0.2 during the measurement. It is important to mention here that zeta potential is not a direct measure of stability but gives an idea of the electrostatic stability of the colloidal system.[27]

Optical Microscopy

Optical microscopy was performed to confirm vesicle formation and evaluate the morphology and distribution of transferosomes before and after drug entrapment. A drop of blank and drug-loaded transferosome suspensions was placed on a clean glass slide and observed under a microscope at 10× and 45× magnifications to assess vesicle formation, particle distribution, and the presence of aggregation or structural changes.[28]

Scanning Electron Microscopy (SEM)

The Scanning Electron Microscopy (SEM) technique was used for the examination of morphological characteristics and size distribution of the transferosomes developed. The samples were prepared in such a way that they could be mounted on SEM stubs and examined using a Zeiss SEM machine with 10.0 kV accelerating voltage and 10.5 mm working distance. The images were captured at 5.00 KX, 15.00 KX, and 20.00 KX magnifications.

Entrapment Efficiency

Entrapment Efficiency (EE%) was calculated to measure the encapsulating potential of the formulated transferosomes. For that purpose, 1 mL of transferosome solution was taken, and diluted in the phosphate buffer (pH 7.4) and then the solution was centrifuged at 15,000-20,000 rpm for 30 min. The separated supernatant was collected, filtered through Whatman filter paper No. 1, diluted again in the phosphate buffer (pH 7.4) and measured on a UV-visible spectrophotometer at 295 nm wavelength. The concentration of free drug was measured from calibration curve, and the entrapment efficiency was calculated by using the formula.[29-31]

$$\%EE = \frac{\text{Total drug} - \text{Free drug}}{\text{Total drug}} \times 100$$

Evaluation of Transferosomal Gel

Physical Appearance, pH, Viscosity, Spreadability, Extrudability, and Washability

Physical appearance was evaluated according to predefined acceptance criteria. Colour, homogeneity, clarity, absence of lumps, grittiness, presence of air bubbles and phase separation were independently evaluated under identical daylight illumination for all the formulations against white and black

backgrounds (n=3). Observations were made qualitatively, either acceptable or unacceptable, depending on the absence of visual defects. The pH value was determined in triplicate using a digital pH meter (1 g of gel dissolved in 10 mL of distilled water). Viscosity was measured using a Brookfield DV-E Digital Viscometer (Brookfield Engineering Laboratories) equipped with spindle S64 at 10 rpm and maintained at 25±0.5°C. Approximately 30 g of gel was placed in the sample container and allowed to equilibrate for 5 min before measurement. Three independent measurements (n=3) were recorded and expressed as mean±SD. The spreadability value was determined as the time required to separate two glass slides under constant pressure, while the extrudability value was determined as the mass of the gel that had been extruded from a collapsible tube under 500 g pressure in 10 sec.

Drug Content

Drug content determination obtain the exact value of drug content present per gram of gel formulation. An exact weighed amount of gel formulation (1 g) was dissolved in methanol, filtrated and then diluted (1:10), and then the absorbance was taken at 295 nm using methanol as blank. Drugs content were determined by calculating the percentage ratio of actual to theoretical drugs content from the equation validation.

FTIR Spectroscopy of the Formulation

The optimised gel formula was characterized by ATR-FTIR (4000-400 cm^{-1}) in order to verify the presence of specific absorption bands of drugs and excipients and eliminate any possibility of chemical reaction/degradation in gel.

In vitro Drug Release and Release Kinetics

The Franz diffusion cell is a standard *in vitro* method for evaluating drug release. A Franz diffusion cell fitted with a pre-hydrated cellulose acetate membrane (0.45 µm) was used for study. The receptor compartment contained 60 mL Phosphate-Buffered Saline (PBS, pH 7.4), maintained at 37±0.5°C with magnetic stirring (100 rpm). The optimized gel (equivalent to 10 mg dapsone) was applied to the donor compartment, and 1 mL aliquots were withdrawn at 0, 0.5, 1, 2, 3, 4, 6, 8, 10, and 12 hr, with immediate replacement by fresh pre-warmed PBS. Withdrawn samples were diluted (10×) and absorbance measured at 295 nm; cumulative percentage drug release (%CDR) was calculated with correction for volume replacement. Drug release data were analysed using DDSolver Version 1.0 (Microsoft Excel add-in). Zero-order, First-order, Higuchi and Korsmeyer-Peppas models were fitted. Model selection was based on the highest coefficient of determination (R^2), highest adjusted R^2, lowest Akaike Information Criterion (AIC), and highest Model Selection Criterion (MSC).[30,31]

Physical stability studies

Stability studies were carried out according to the International Council for Harmonisation (ICH) guideline Q1A(R^2). The optimized formulation was then kept at room temperature (25°C/60% RH) and refrigerated temperature (4-6°C) for 45 days. At predetermined time points (0, 15, and 45 days), samples were taken and analyzed with respect to physical appearance, drug content, and entrapment efficiency.[27]

Antioxidant Activity (DPPH Radical Scavenging Assay)

Acne vulgaris has been closely associated with oxidative stress, wherein excess free radicals trigger lipid peroxidation and amplify the inflammatory cascade in the pilosebaceous unit. Antioxidants neutralise these Reactive Oxygen Species (ROS), thereby suppressing pro-inflammatory mediators (IL-1β, TNF-α) and reducing the severity of inflammatory acne lesions. The free-radical scavenging potential of the optimized transferosome gel (designated AVS01) was evaluated by the DPPH assay, benchmarked against ascorbic acid as standard. A freshly prepared 0.1 mM DPPH solution in methanol was mixed with test samples (ascorbic acid at 2-10 µg/mL; gel at 1000-1400 µL) and incubated for 30 min in the dark at room temperature. The absorbance was measured at 517 nm, and the % inhibition was computed as [(A control - A sample)/A control] × 100.

Antibacterial Activity (Agar Well Diffusion Method)

The antibacterial activity of the optimized Dapsone transferosomal gel was evaluated to assess its efficacy against acne-associated microorganisms using the agar well diffusion method. Sterile agar medium was prepared, poured into Petri dishes, and inoculated with freshly prepared cultures of *Staphylococcus aureus* and *Escherichia coli* adjusted to 0.5 McFarland standard. Wells of 6 mm diameter were made in the agar plates and loaded with 100 µg of the optimized Dapsone transferosomal gel, marketed gel (Acnesol®), and normal saline as a negative control. The plates were incubated at 37°C for 24 hr after being held at 4°C for 1 hr to facilitate in pre-diffusion. The zones of inhibition were measured in millimeters after incubation and recorded to measure the formulations' antibacterial effectiveness. Despite Acne Vulgaris being predominantly caused by *C. acnes* bacteria,

Table 1: Independent Variables (Factors) in the Box-Behnken Design.

Factor	Name	Units	Low (-1)	Centre (0)	High (+1)
A	Lipid	mg	100	150	200
B	Edge activator (Span 80)	mg	20	25	30
C	Chloroform: Methanol ratio	% v/v	1.2	1.5	1.8

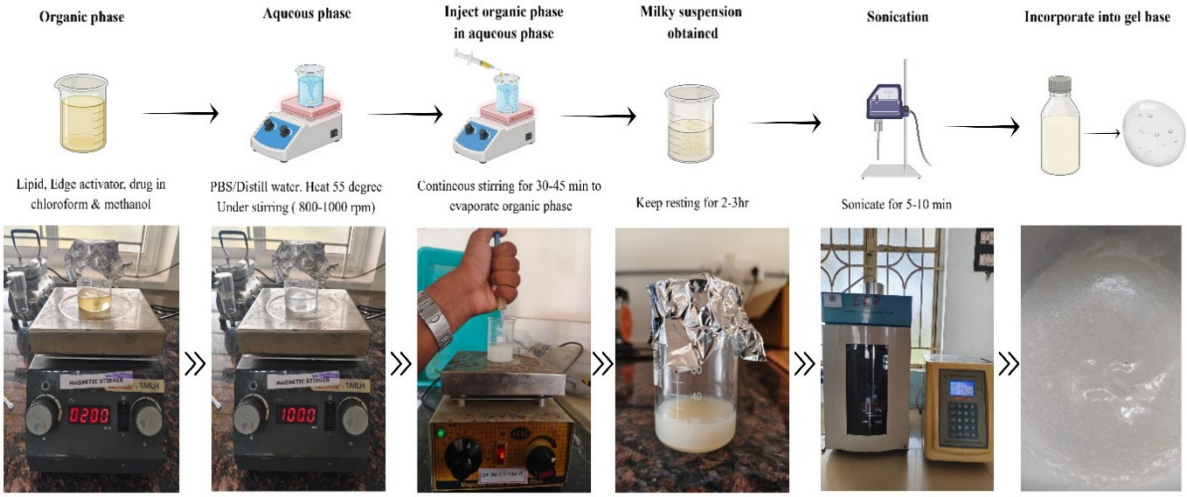


Figure 1: Schematic Representation of the Preparation of Dapsone Transferosomal Gel.

the antibacterial testing was conducted utilizing *Staphylococcus aureus* and *Escherichia coli* bacteria, which were chosen as models for Gram-positive and Gram-negative bacteria respectively due to their availability and frequent use in the initial antimicrobial testing of topical drugs.

Ethical Approval

This article does not contain any studies involving human participants or animals performed by any of the authors.

Statistical Analysis

The data obtained from the optimized transferosomal gel were presented as means±Standard Deviation (SD) for triplicate experiments (n=3). The statistical analysis and response-surface methodology were accomplished by the software Design-Expert 13®, designed for the Box-Behnken design. The significance of the fitted models and individual factors was determined by Analysis of Variance (ANOVA) with p value<0.05 being statistically significant.

RESULTS

Wavelength of Maximum Absorption (λ_{max}) and Calibration Curve

UV-visible spectral scanning of dapsone over 200-400 nm revealed a well-defined absorption maximum at 295 nm, which was adopted as λ_{max} for all subsequent spectrophotometric estimations (Figure 2). Over the concentration range of 2-10 µg/mL, a linear calibration curve was produced (Figure 3). yielding the regression equation y=0.066x with a coefficient of determination R^2=0.999, confirming excellent linearity and method suitability for quantitative estimation of dapsone throughout the study.

FTIR Compatibility Study

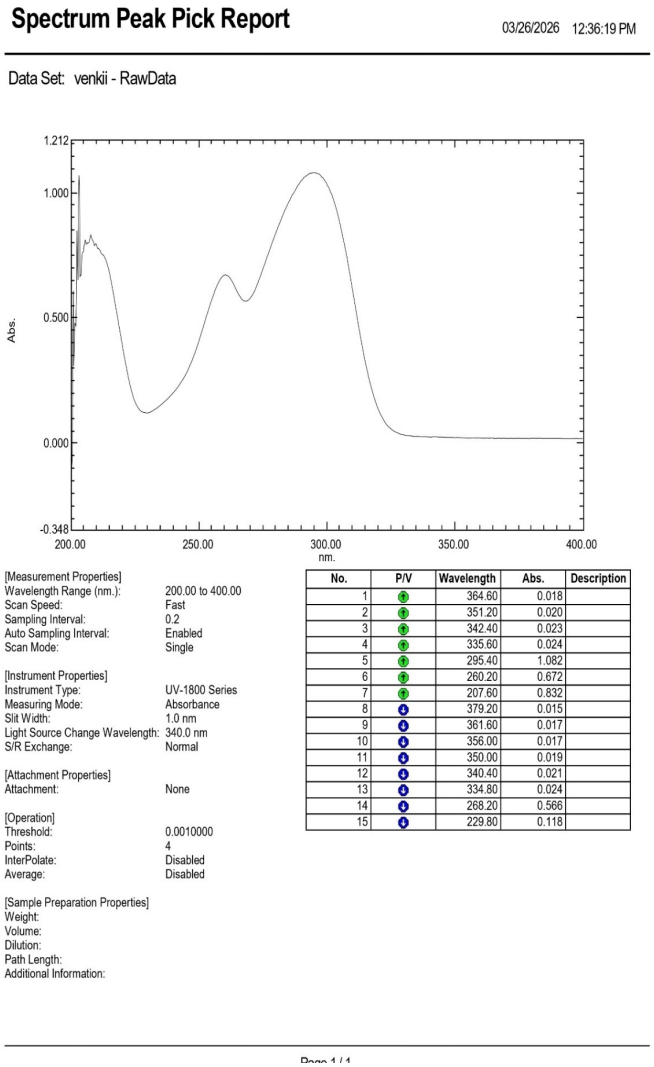
The FTIR spectrum of pure dapsone exhibited characteristic peaks corresponding to aromatic N-H stretching (3334.65 and 3359.06 cm^{-1}), aromatic C-H stretching (3064.66 cm^{-1}), and asymmetric and symmetric sulfone S=O stretching vibrations (1338.45 and 1184.79 cm^{-1}), confirming its characteristic diaryl sulfone structure. Soya lecithin and Span 80 showed characteristic ester carbonyl (C=O) stretching bands at 1734.82 and 1736.26 cm^{-1}, respectively. There were no notable chemical interactions, as shown by the physical mixture's FTIR spectrum retaining all of the major characteristic peaks of the individual components with only slight shifts. These findings confirm the physicochemical compatibility of dapsone with soya lecithin and Span 80, supporting their suitability for transferosomal formulation development. The FTIR spectra of dapsone, soya lecithin, Span 80, and their physical mixture are presented in Figure 4.

Box-Behnken Design Optimization of Dapsone Transferosomal Gel

Box-Behnken design produced 17 formulations within the design space constituted by lipid concentration, edge activator concentration, and chloroform: methanol ratio. During the process, vesicle size was between 205 nm and 245 nm; encapsulation efficiency was from 78.8% to 84.2%; zeta potential was from -31.5 mV to -30.0 mV; and drug release was from 85.5% to 89.2% (Table 2), thus ensuring that a broad response surface is obtained within the selected range of factors. Replication of centre point (runs 13-17) ensured minimal variability.

ANOVA and Statistical Model Fitting

All the quadratic polynomial models for all the responses tested proved to be significant (p<0.05) with non-significant lack-of-fit in each case, indicating an adequate fit for the data (Table 3).



Spectrum Peak Pick Report

03/26/2026 12:36:19 PM

Data Set: venkii - RawData

[Measurement Properties]
Wavelength Range (nm.): 200.00 to 400.00
Scan Speed: Fast
Sampling Interval: 0.2
Auto Sampling Interval: Enabled
Scan Mode: Single

[Instrument Properties]
Instrument Type: UV-1800 Series
Measuring Mode: Absorbance
Slit Width: 1.0 nm
Light Source Change Wavelength: 340.0 nm
S/R Exchange: Normal

[Attachment Properties]
Attachment: None

[Operation]
Threshold: 0.0010000
Points: 4
InterPolate: Disabled
Average: Disabled

[Sample Preparation Properties]
Weight:
Volume:
Dilution:
Path Length:
Additional Information:

No.	P/V	Wavelength	Abs.	Description
1	↑	364.60	0.018	
2	↑	351.20	0.020	
3	↑	342.40	0.023	
4	↑	335.60	0.024	
5	↑	295.40	1.082	
6	↑	260.20	0.672	
7	↑	207.60	0.832	
8	↓	379.20	0.015	
9	↓	361.60	0.017	
10	↓	356.00	0.017	
11	↓	350.00	0.019	
12	↓	340.40	0.021	
13	↓	334.80	0.024	
14	↓	268.20	0.566	
15	↓	229.80	0.118	

Figure 2: UV-visible absorption spectrum of Dapsone showing λ_{max}=295 nm.

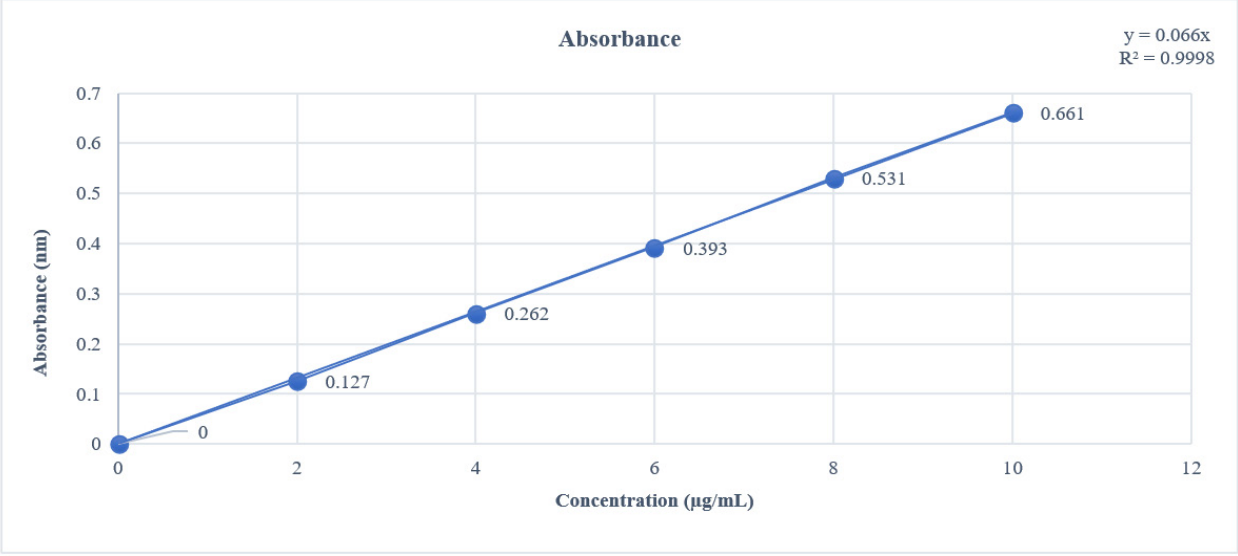


Figure 3: Standard calibration curve of Dapsone and table.

Table 2: Box-Behnken Design Matrix with Observed Responses.

Run	A: Lipid (mg)	B: Edge Activator (mg)	C: Chloroform: Methanol Ratio	Vesicle Size (nm) (nm)	Entrapment Efficiency (%)	Zeta Potential (mV)	Drug Release (%)
1	100	20	1.2	205	79.5	-30.5	86.5
2	200	20	1.2	230	78.8	-31.0	85.5
3	100	30	1.2	210	80.2	-30.8	87.0
4	200	30	1.2	240	81.0	-31.5	86.0
5	100	20	1.6	208	80.0	-30.2	87.0
6	200	20	1.5	235	79.2	-30.8	86.0
7	100	30	1.5	212	81.0	-30.5	87.5
8	200	30	1.5	245	82.0	-31.2	86.5
9	100	25	1.5	210	83.0	-30.0	88.5
10	200	25	1.6	240	82.0	-31.0	87.5
11	150	20	1.5	225	80.5	-30.8	86.5
12	150	30	1.5	238	82.0	-31.2	87.2
13	150	25	1.2	230	83.5	-30.2	88.8
14	150	25	1.8	235	83.2	-30.5	88.6
15	150	25	1.5	232	84.0	-30.5	89.0
16	150	25	1.5	233	83.8	-30.4	88.8
17	150	25	1.5	231	84.2	-30.6	89.2

Table 3: ANOVA Summary for Quadratic Models of All Responses.

Source/Statistic	Vs (nm)	EE (%)	ZP (mV)	DR (%)
Model (p)	<0.0001	<0.0001	0.0144	0.0001
A - Lipid (p)	<0.0001	0.2804 (NS)	0.0016	0.0027
B - EA (p)	0.0001	0.0003	0.0591 (NS)	0.0601 (NS)
C - CM:ML (p)	0.0109	0.4303 (NS)	0.9402 (NS)	0.9577 (NS)
Lack of fit (p)	0.2794 (NS)	0.2385 (NS)	0.1574 (NS)	0.2758 (NS)
R^2	0.9939	0.9846	0.8837	0.9709
Adjusted R^2	0.9860	0.9649	0.7342	0.9335
Adequate precision	34.22	19.91	9.016	14.054

Vesicle-size was modeled using a significant (F=126.18, p<0.0001; R^2=0.9939) model with lipid concentration (A) being the most significant factor (F=678.37, p<0.0001). The encapsulation efficiency model was significant (F = 49.81, p<0.0001; R^2=0.9846) with the edge-activator (B) being the most significant factor (p=0.0003). The zeta potential model proved to be significant (F=5.91, p=0.014; R^2=0.8837) with relatively poor predictive ability (predicted R^2=-0.027) but with adequate precision (9.016). The drug-release model was significant (F=25.96, p=0.0001; R^2=0.9709), driven by lipid concentration and the quadratic B^2 term.

Response and surface analysis

Three-dimensional surface plots were used to demonstrate the interactive effects of the lipid concentration and edge activator concentration on each response variable (Figure 5). The size of the vesicles increased sharply and linearly with increasing lipid concentration, ranging between 205 nm and 245 nm for the whole design region. This could be attributed to increased membrane mass and development of multilamellar vesicles due to high lipid loading. The surface response plot for encapsulation efficiency was dome-shaped, and it was maximized at medium-to-low lipid concentration and medium edge activator concentration. This can be attributed to excess surfactant causing destabilization of the vesicles and hence drug leakage.

Perturbation, Interaction, and Contour Plot Analysis

Perturbation plots were used to analyze the individual effect of the formulation variables on the responses and it was found that lipid concentration had the strongest effect on vesicle size and

drug release, while edge activator concentration had an important effect on entrapment efficiency. Two-factor interaction plots depicted the synergistic and quadratic interaction effect of the lipid concentration, edge activator concentration and chloroform: methanol ratio, proving that these formulation variables have a significant effect on the CQAs of the transferosomal formulation. Contour plots further analyzed the design space and provided information about the optimum region based on low lipid concentration, moderate edge activator concentration and moderate solvent ratio, yielding nanosized vesicles with improved entrapment efficiency and controlled drug release. Nonlinearity and interaction of variables in the formulation optimization were thus proved, making the Box-Behnken design suitable for optimizing the formulation of the transferosomes. The figures used in this analysis include Perturbation Plots, Two-Factor Interaction Plots and Two-Dimensional Contour Plots designed using the Design-Expert® software. The perturbation, interaction and contour plots are shown in Figure 6.

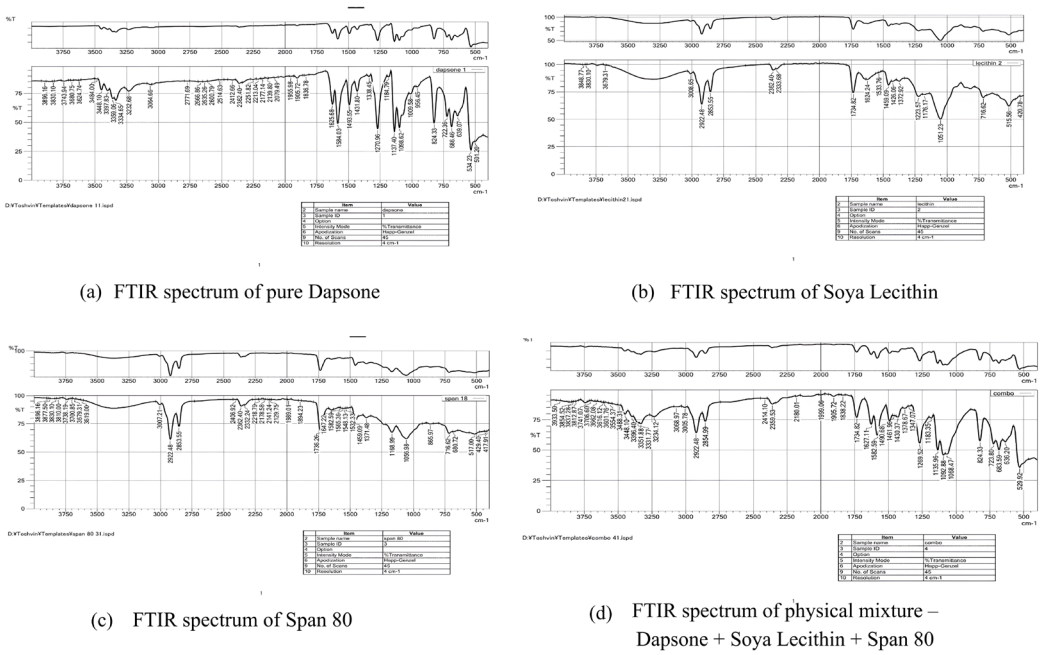
Numerical Optimization and Validation of the Optimized Formulation

The optimisation process was performed simultaneously by applying the method of the desirability function with constraints that reduce the vesicle size while increasing the encapsulation efficiency, zeta potential, and drug release as observed in the range of the design. Solution having highest desirability value (0.885) was selected as the optimal formulation with lipid concentration of 100.00 mg, edge-activator concentration of 25.20 mg, and chloroform:methanol ratio of 1.48. (Table 4).

Optimised formulation was prepared as per the predicted factor levels and evaluated through experimentation. High degree of concurrence of predicted and experimental results (error in prediction < 5%) confirmed the reliability of Box-Behnken equation. Hence, it can be said that Box-Behnken design efficiently modeled the nonlinear and interactive effects of the factors on the quality parameters of transferosomes. Among the three factors analyzed, lipid concentration appeared to be the most dominating factor affecting vesicle size, whereas edge-activator concentration exhibited maximum effect on encapsulation efficiency and drug release, implying that the optimal formulation process consists of lower lipid concentration along with medium level of edge-activator concentration.

Table 4: Numerical Optimization Results and Predicted Responses of the Optimized Dapsone Transferosomal Formulation.

Parameter	Optimized Value	Goal
A: Lipid concentration	100.00 mg	In range
B: Edge activator concentration	25.20 mg	In range
C: Chloroform:Methanol ratio	1.48	In range
R^1: Vesicle size (Vs)	209.92 nm	Minimize
R^2: Encapsulation efficiency (EE)	82.99%	Maximize
R^3: Zeta potential (ZP)	-30.00 mV	Maximize
R^4: Drug release (DR)	88.83%	Maximize
Overall desirability	0.885	—



(a) FTIR spectrum of pure Dapsone

(b) FTIR spectrum of Soya Lecithin

(c) FTIR spectrum of Span 80

(d) FTIR spectrum of physical mixture – Dapsone + Soya Lecithin + Span 80

Figure 4: FTIR spectra of dapsone (a), soya lecithin (b), Span 80 (c), and physical mixture (d).

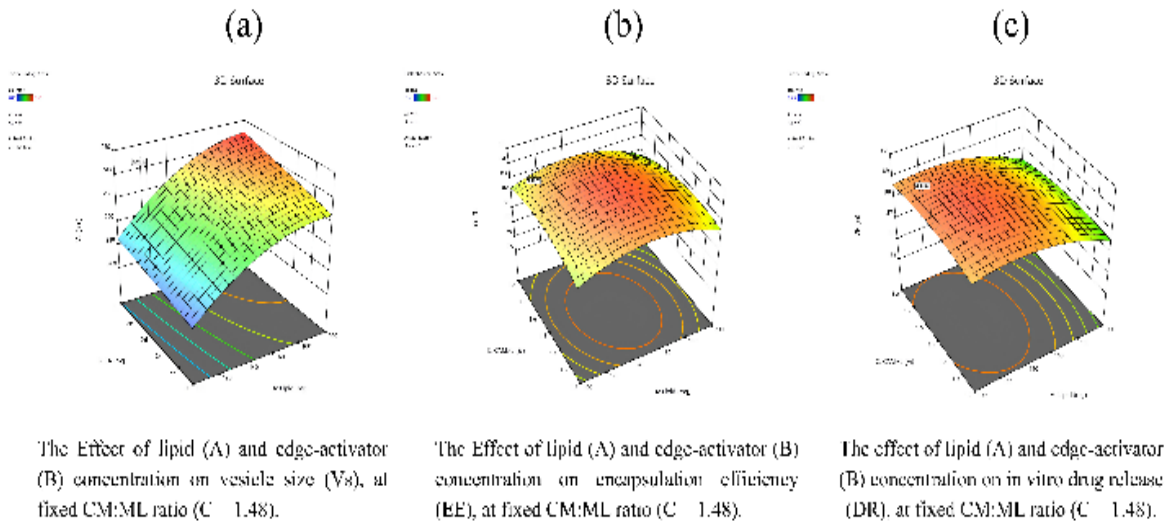


Figure 5: Three-Dimensional Response Surface Plot Showing the Effect of Lipid and Edge Activator on Vesicle Size (a), Effect of Formulation Variables on Entrapment Efficiency (b), Effect of Formulation Variables on Drug Release (c).

Table 5: Entrapment Efficiency Parameters and Percentage Drug Encapsulation of Optimized Dapsone Transferosomes.

Parameter	Value
Absorbance measured (λ_{max}=295 nm)	0.259
Calibration equation	y=0.066x
R^2 value	0.999
Concentration in diluted solution	3.924 µg/mL
Overall dilution factor	20×
Free drug concentration (original suspension)	78.48 µg/mL
Total free drug (20 mL batch)	1.5697 mg
Total drug incorporated	10 mg
Entrapped drug	8.4303 mg
Entrapment Efficiency (%EE)	84.30%

Characterization of the Optimized Transferosomes

Particle Size and Polydispersity Index (PDI)

The Dynamic Light Scattering of the optimized formulation of the transferosomes yielded a mean hydrodynamic diameter of 210.0 nm using the Cumulants technique, which had a Polydispersity Index (PDI) value of 0.307 (showing that the vesicles are moderately polydisperse (Figure 7). The value of D (10%), D (50%), and D (90%) were 85.80, 250.70, and 770.60 nm, respectively. There was a good correlation between the experimental value of the size of the vesicle and the predicted value using the Box-Behnken model (209.92 nm)

Zeta Potential

Zeta potential of the developed formulation was determined to be -30.6 mV (standard deviation 4.9 mV), which showed a highly symmetric and singular peak with 100% area contribution (Figure 8) and was very close to that predicted by Box-Behnken model (-30.00 mV). The moderately high negative surface charge associated with the phospholipid headgroups ensures enough repulsive forces among vesicles for the stabilization of the system.

Scanning Electron Microscopy

SEM analysis of the optimized transferosomes revealed particles with an angular-to-sub-rounded morphology and a porous, granular surface texture characteristic of lipid-based vesicular systems (Figure 9). Particle sizes observed under SEM, spanning sub-micron to micron dimensions across different magnifications (5.00-20.00 KX), were in general agreement with the hydrodynamic diameter obtained by DLS, supporting successful formation of discrete vesicular transferosomes with morphology consistent with efficient transdermal/topical permeation potential.

Entrapment Efficiency

The entrapment efficiency of the optimized transferosomal formulation, determined by the indirect method, was 84.30% (Table 5), closely matching the Box-Behnken model prediction (82.99%) and falling well within the acceptable range reported for transferosomal systems (70-95%). This satisfactory entrapment is attributable to the amphiphilic character of dapsone, which favours partitioning into the lipid bilayer, augmented by the membrane-flexibilizing action of the Span 80 edge activator.

Evaluation of the Transferosomal Gel

Physical Appearance and Optical Microscopy

The optimized gel met all the pre-defined acceptance criteria. Both the appearance of the product, and the absence of phase separation, lumping, grittiness or air bubbles, were uniform for all three batches throughout the evaluation period (Figure 10). Optical microscopy of the dapsone-loaded transferosome gel confirmed uniform dispersion of small, spherical vesicular

structures throughout the gel matrix, with no evidence of fusion or aggregation, indicating successful and stable incorporation of the transferosomes into the semi-solid dosage form.

FTIR Spectroscopy of the Gel Formulation

FTIR analysis of the optimized gel formulation (Figure 11) confirmed retention of all principal diagnostic absorption bands of dapsone, soya lecithin, and Span 80, including the dapsone N-H stretch at 3343.26 cm^{-1}, the sulfone S=O stretches at 1334.15 and 1225.00 cm^{-1}, and the lecithin ester carbonyl C=O stretch at 1734.82 cm^{-1}, with no appearance of new peaks or significant band disappearance. The minor wavenumber shifts (≤5-10 cm^{-1}) observed are consistent with increased intermolecular hydrogen bonding within the viscoelastic gel matrix rather than chemical incompatibility, confirming that dapsone remains chemically stable within the transferosomal gel.

Drug Content

The drug content of the optimized gel was 9.696 mg per 20 g batch, corresponding to a recovery of 96.96% relative to the theoretical drug loading (Table 6), confirming accurate and uniform incorporation of dapsone during formulation and supporting the reliability of the analytical method employed.

Physicochemical Evaluation Summary

All physicochemical properties necessary for a semi-solid dosage form were achieved in the optimized formulation (Table 7). It had a pH value (6.69±0.015) close to skin pH and low chances of irritation; its viscosity (3836.67±15.28 cP) was suitable for ease of application and prolonged skin residence; spreadability (7.00±0.00 s) and extrudability (0.71±0.01 g/500g/10 s) were among desirable properties.

In vitro Drug Release and Release Kinetics

In vitro Drug release

The optimized transferosomal gel was observed to exhibit sustained drug release with almost complete drug release of 88.10±0.33% after 12 hr (Table 8), which is in close to the predicted value obtained from the Box-Behnken model (88.83%),

Table 6: Drug Content Analysis of the Optimized Gel.

Parameter	Value
Absorbance at λ_{max} (295 nm)	0.032
Drug content per gram of gel	0.4848 mg/g
Drug content (20 g batch)	9.696 mg
Theoretical drug added	10 mg
% Drug recovery	96.96%

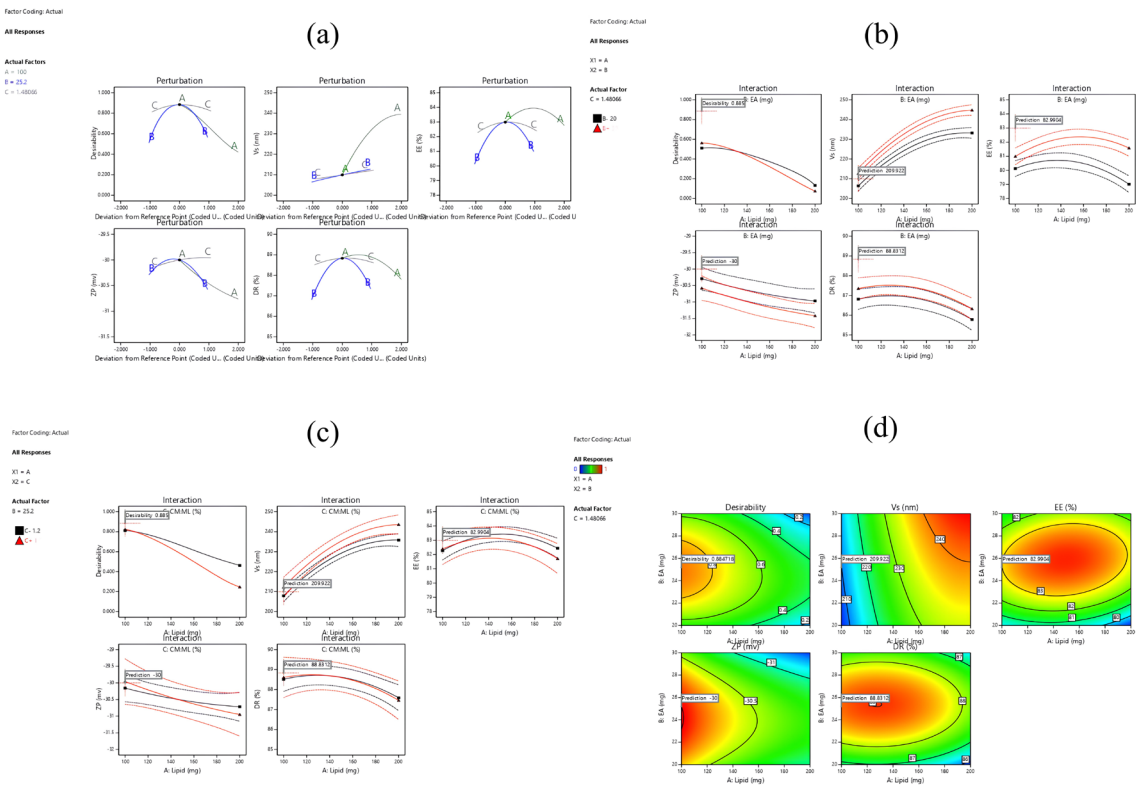


Figure 6: Perturbation Plot (a), Interaction plot (b, c), Contour plot of optimized formulation (d).

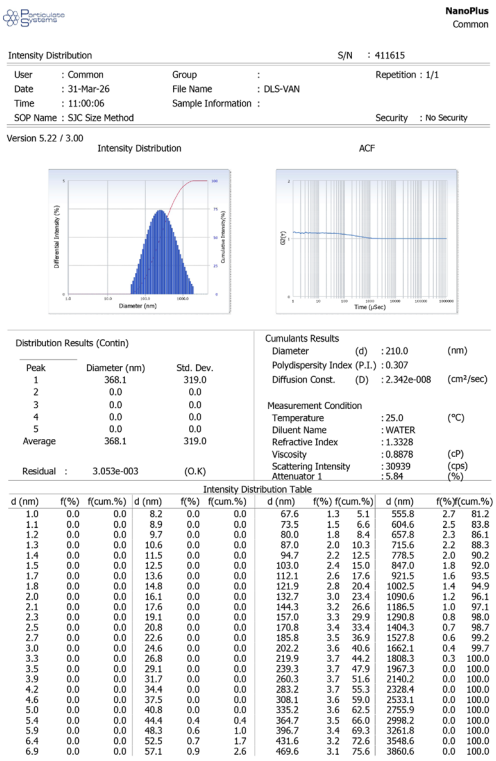


Figure 7: Particle Size Distribution and Polydispersity Index (PDI) of Optimized Transferosomes.

Table 7: Summary of Gel Evaluation Parameters.

Parameter	Result (Mean±SD)	Inference
Physical appearance	Dark grey, opaque, smooth, homogeneous	Satisfactory
pH	6.69±0.015	Acceptable
Viscosity	3836.67±15.28 cP	Satisfactory
Spreadability	7.00±0.00 sec	Good
Extrudability	0.71±0.01 g / 500 g / 10 s	Good
Washability	Complete removal with water	Excellent

thereby establishing controlled drug release. The cumulative drug release profiles of all formulations and the optimized formulation are shown in Figure 12. The cumulative drug release data for all seventeen Box-Behnken formulations are summarized in Table 9.

Release Kinetics

The release data were fitted to Zero-Order, First-Order, Higuchi, and Korsmeyer-Peppas kinetic models using DDSolver software (Table 10). Based on the highest R^2 (0.9937), most negative AIC (-48.66), and highest MSC (4.40), the Korsmeyer-Peppas model provided the best fit to the release profile. The corresponding release exponent (n=0.635, falling between 0.45 and 0.89) indicated anomalous, non-Fickian transport, suggesting that drug

Table 8: *In vitro* Cumulative Drug Release of Dapsone from the Optimized Transferosomal Gel (n=3, Mean±SD).

Time (hr)	Mean %CDR±SD
0	0.00±0.00
0.5	8.20±0.14
1	15.60±0.31
2	26.80±0.23
3	38.40±0.35
4	47.90±0.25
6	59.20±0.35
8	67.80±0.39
10	76.30±0.17
12	88.10±0.33

release from the optimized gel occurs through a combination of diffusion through the lipid bilayer/gel matrix and polymer chain relaxation, consistent with the behaviour expected of a hydrophilic Carbopol-based matrix embedding deformable vesicular carriers. The release kinetic plots obtained from DDSolver are presented in Figure 13.

Drug release kinetic modeling was performed to evaluate the mechanism and pattern of dapsone release from the optimized transferosomal gel formulation. The *in vitro* release data were fitted into various mathematical models using DDSolver Version

1.0 to determine the best-fit release kinetics and transport mechanism.

Among all evaluated models, the Korsmeyer-Peppas model demonstrated the highest R^2 (0.9937), highest MSC (4.40), and lowest AIC (-48.66), indicating the best statistical fit. The release exponent (n=0.635) confirmed anomalous (non-Fickian) diffusion involving both diffusion and polymer relaxation mechanisms. Therefore, the optimized dapsone transferosomal gel exhibited a sustained release profile governed by a combination of diffusion through the gel matrix and polymer relaxation, which is characteristic of vesicular drug delivery systems.

Physical stability studies

The physical stability of the optimized dapsone-loaded transferosomal gel (F-opt) was evaluated over a period of 45 days at two storage conditions: refrigerator temperature (4-6°C) and room temperature (25°C /60% RH). The stability parameters assessed included physical appearance, drug content (%), and Entrapment Efficiency (EE%). The results are summarized in Table 11.

The physical stability assessment revealed that the optimized dapsone-loaded transferosomal gel retained its clear appearance, drug content, and entrapment efficiency with no significant degradation over 45 days at both refrigerator (4-6°C) and room temperature (25°C /60% RH) conditions, demonstrating the robustness of the vesicular bilayer in preserving drug integrity. The marginally greater retention of EE% and drug content observed under refrigerator storage compared to room temperature further affirms that cold storage minimizes membrane fluidity and drug leakage, thereby enhancing the long-term stability of the transferosomal formulation.

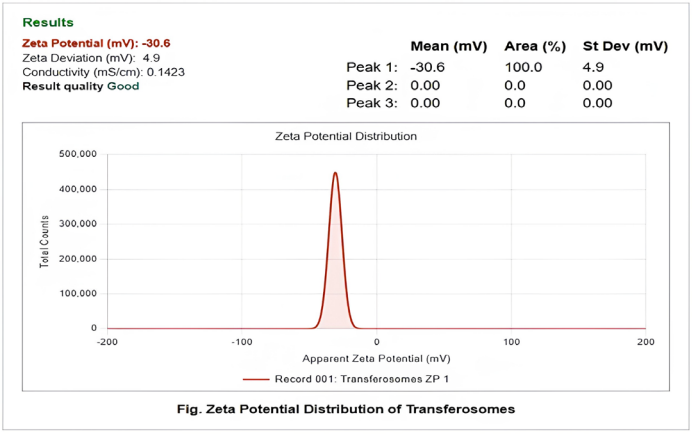


Figure 8: Zeta Potential Distribution of Optimized Dapsone Transferosomes.

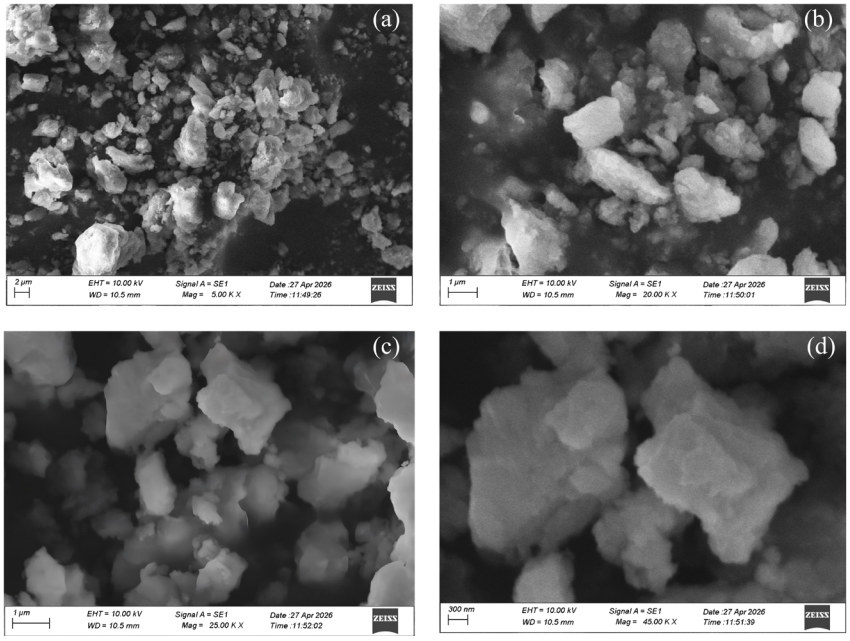


Figure 9: Scanning Electron Micrographs of Optimized Transferosomes at Different Magnifications.

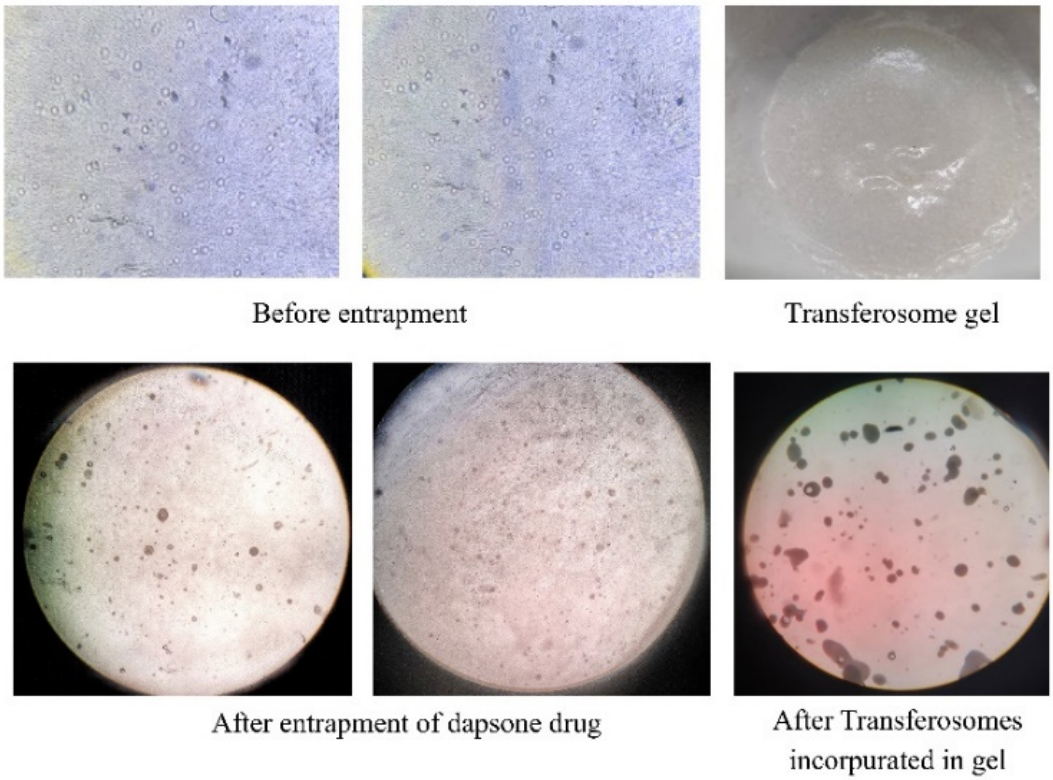


Figure 10: Optical Microscopic Image of Dapsone-Loaded Transferosomal Gel Showing Uniform Vesicular Distribution and Photograph of Optimized Dapsone Transferosomal Gel Showing Physical Appearance.

Table 9: Cumulative % Drug Release (Mean, *n*=3) at 0, 0.5, 1, 2, 3, 4, 6, 8, 10 and 12 hr - All 17 BBD Formulations.

Std	Run	0 hr	0.5 hr	1 hr	2 hr	3 hr	4 hr	6 hr	8 hr	10 hr	12 hr
10	1	0.00	16.86	26.70	40.69	50.74	58.46	69.60	77.18	82.56	86.50
13	2	0.00	16.31	25.88	39.57	49.48	57.14	68.28	75.94	81.44	85.50
14	3	0.00	17.15	27.13	41.27	51.39	59.14	70.27	77.80	83.13	87.00
5	4	0.00	16.58	26.28	40.12	50.10	57.79	68.93	76.56	82.00	86.00
15	5	0.00	17.15	27.13	41.27	51.39	59.14	70.27	77.80	83.13	87.00
3	6	0.00	16.58	26.28	40.12	50.10	57.79	68.93	76.56	82.00	86.00
16	7	0.00	17.45	27.57	41.87	52.06	59.84	70.96	78.44	83.69	87.50
1	8	0.00	16.86	26.70	40.69	50.74	58.46	69.60	77.18	82.56	86.50
6	9	0.00	18.08	28.50	43.12	53.45	61.28	72.36	79.72	84.84	88.50
7	10	0.00	17.45	27.57	41.87	52.06	59.84	70.96	78.44	83.69	87.50
11	11	0.00	16.86	26.70	40.69	50.74	58.46	69.60	77.18	82.56	86.50
9	12	0.00	17.27	27.30	41.51	51.66	59.42	70.55	78.06	83.35	87.20
2	13	0.00	18.28	28.79	43.51	53.88	61.73	72.79	80.12	85.18	88.80
17	14	0.00	18.15	28.60	43.25	53.59	61.43	72.51	79.85	84.95	88.60
4	15	0.00	18.42	28.99	43.77	54.18	62.03	73.08	80.38	85.41	89.00
12	16	0.00	18.28	28.79	43.51	53.88	61.73	72.79	80.12	85.18	88.80
8	17	0.00	18.56	29.19	44.04	54.47	62.33	73.38	80.64	85.65	89.20

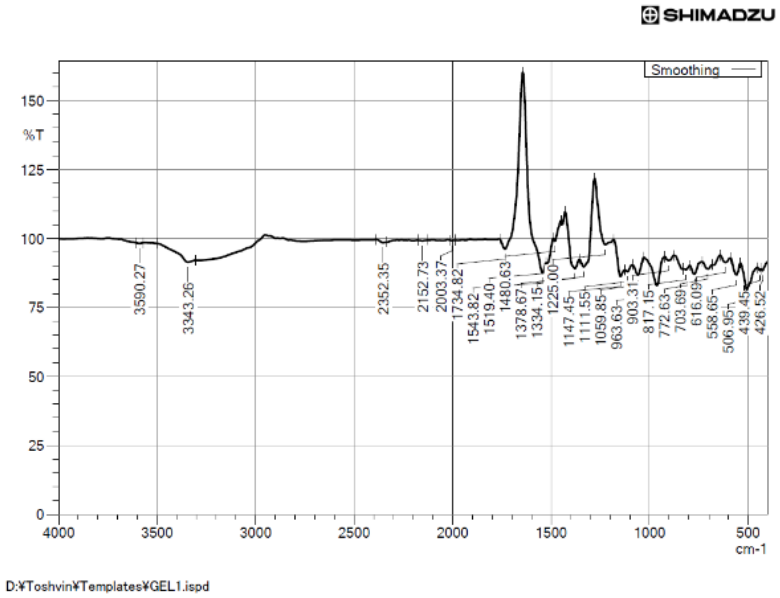


Figure 11: FT-IR Spectrum of Transferosome gel.

Table 10: Goodness-of-Fit Statistics for Release Kinetic Models.

Parameter	Zero-Order	First-Order	Higuchi	Korsmeyer-Peppas
R^2	0.8969	0.8981	0.9716	0.9937
AIC	-22.78	-22.89	-35.69	-48.66
MSC	1.82	1.83	3.11	4.40

Table 11: Stability study results of optimized dapsone-loaded transferosomal gel.

Time point	Physical appearance	Drug content (%)	Entrapment efficiency (%)
Refrigerator condition (4-6°C)			
Day 0	Clear	96.96±0.18	84.30±0.22
15 days	Clear	96.84±0.21	84.10±0.19
45 days	Clear	96.91±0.15	84.35±0.24
Room temperature (25°C / 60% RH)			
Day 0	Clear	96.96±0.18	84.30±0.22
15 days	Clear	95.89±0.27	83.22±0.31
45 days	Clear	95.43±0.33	82.96±0.28

Antioxidant Activity (DPPH Radical Scavenging Assay)

The concentration-dependent activity against DPPH radicals was observed in the case of optimized transferosomal gel (AVS01), as the percent of inhibition increased from 20.83% to 70.83% at different concentrations of the formulation (1000-1400 µL) (Table 12 and Figure 14). The standard used, that is ascorbic acid, also had similar concentration-dependent activity (percent inhibition=11.1 to 72.3% between 2 and 10 µg/mL), with the good linearity in both the cases (ascorbic acid: y=7.5405x - 4.5037, R^2=0.9975), confirming assay reliability.

The maximum inhibition of the transferosomal gel (70.83% at 1400 µL) was very much similar to the inhibition by the ascorbic acid standard at its maximum concentration (72.3% at 10 µg/mL). This shows that the optimized transferosomal gel contains a high level of antioxidant effect, which plays a significant role in the mechanism of action of the transferosomal gel against acne because of its ability to scavenge reactive oxygen species produced by the inflammation of pilosebaceous unit, hence suppressing

the Inflammatory response (IL-1β and TNF-α) implicated in acne lesion severity, thereby supporting its proposed dual anti-inflammatory/antioxidant role in topical acne management.

Antibacterial Activity

The optimized dapsone transferosomal gel demonstrated superior antibacterial activity against both *Staphylococcus aureus* and *Escherichia coli* in comparison to the marketed reference gel. Against S. aureus, the formulation produced a zone of inhibition of 20.5±0.3 mm, which was greater than that of Acnedep gel (18.7±0.4 mm) and the negative control No zone of inhibition. Similarly, against E. coli, the optimized formulation showed a zone of inhibition of 18.2±0.4 mm, exceeding that of the marketed gel (15.8±0.5 mm), while the negative control showed no inhibition. The enhanced antibacterial activity may be attributed to the deformable transferosomal vesicles, which improve drug penetration and provide sustained localized delivery, thereby enhancing the efficacy of dapsone against both gram-positive and gram-negative bacteria. Representative antibacterial activity images are shown in Figure 15. The antibacterial activity results, expressed as the zone of inhibition, are summarized in Table 13.

DISCUSSION

The Box-Behnken design, the concentrations of lipid and edge-activator were modeled as having significant non-linear effects on the quality attributes of transferosomes, lipid concentration showing a significant effect on vesicle size, and edge-activator concentration on encapsulation efficiency and drug release, which corresponds to the role of the surfactant as a membrane-flexibilizer. The optimized formulation was nanoscale in size, highly negatively charged zeta potential, and an ideal entrapment efficiency, all of which suggest it is a colloidally stable system for targeting the follicles. The FTIR confirmed that there were no interactions between the drugs and excipients, which supports the formulation integrity. The non-Fickian release data suggest that both diffusion and the relaxation of the matrix are involved, which would be more advantageous for sustained drug delivery at the cutaneous level than for the conventional dapsone formulations. The superior antibacterial activity compared to the marketed reference gel and remarkable antioxidant activity indicates possible synergistic antimicrobial and anti-inflammatory effects desirable for acne treatment. sustained stability, especially in refrigerated conditions. These observations highlight the transferosomal gel as a promising

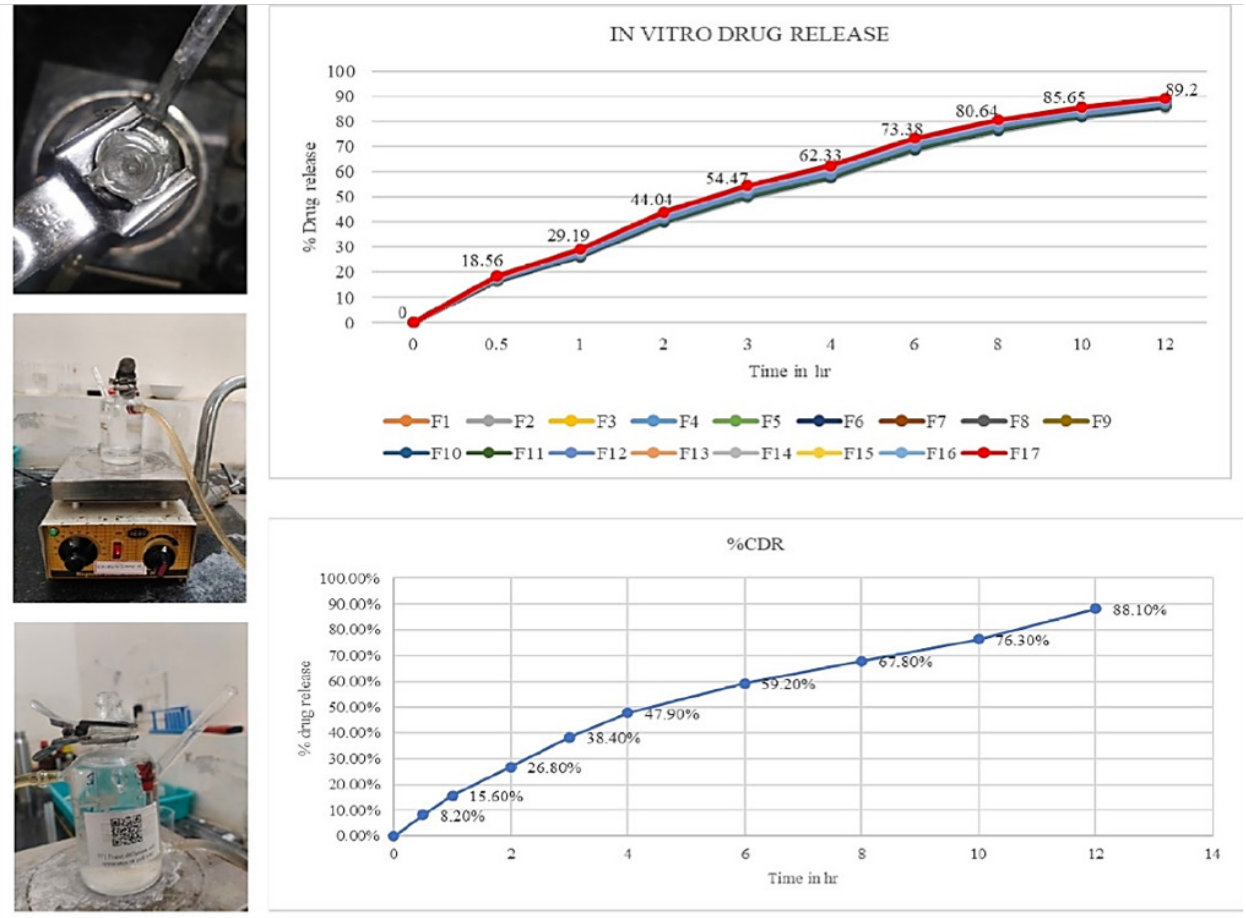


Figure 12: *In vitro* Cumulative Drug Release Profile of 17 and optimized Dapsone Transferosomal Gel.

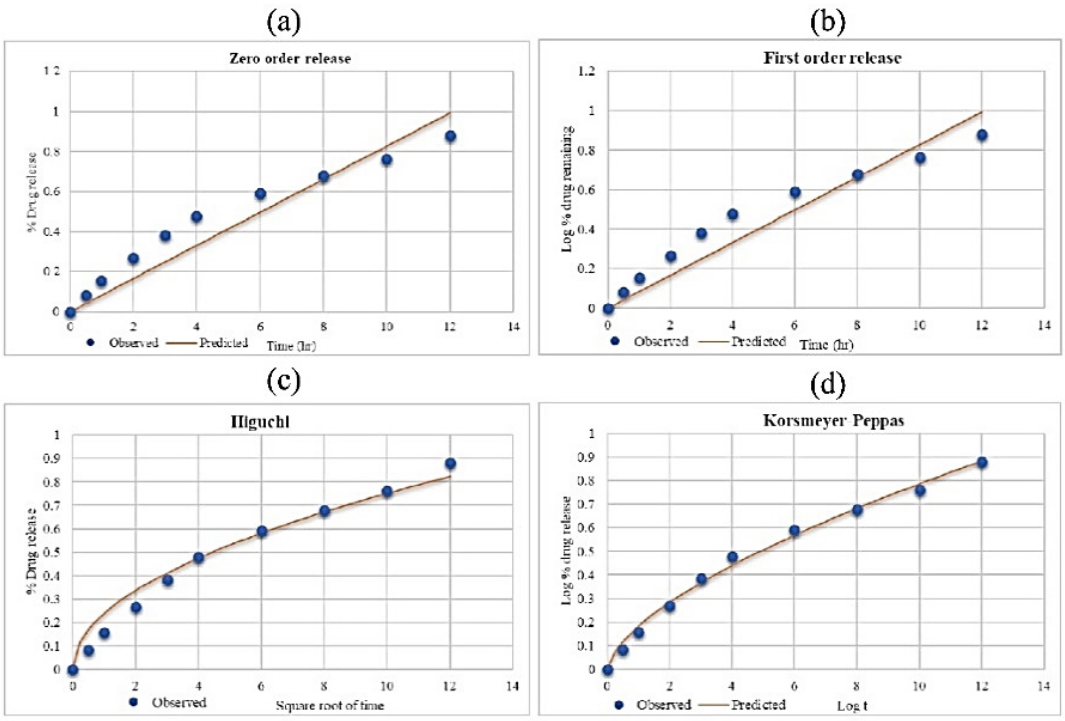


Figure 13: Release Kinetic Model Fitting of Dapsone Transferosomal Gel.

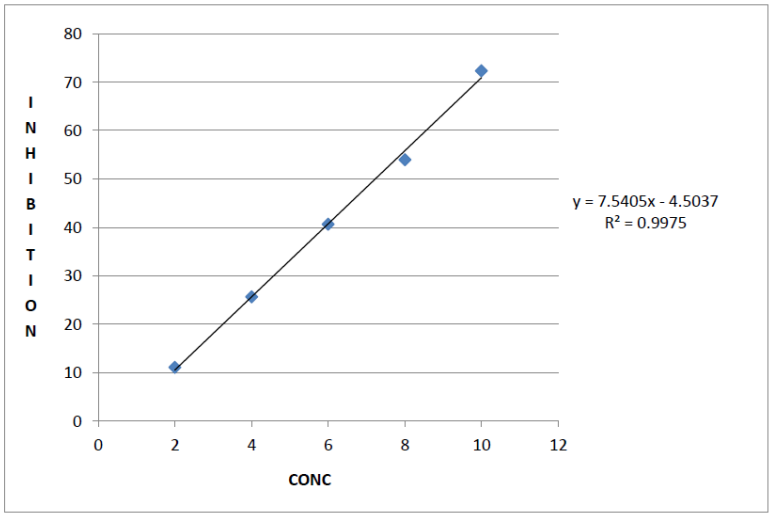


Figure 14: *In vitro* DPPH radical scavenging activity of the optimized dapsone transferosomal gel (AVS01).

Table 12: DPPH Radical Scavenging Activity of Ascorbic Acid (Standard) and Transferosome Gel (AVS01).

Ascorbic Acid Conc. (µg/mL)	% Inhibition (Standard)	Gel Conc. (µL)	% Inhibition (AVS01)
2	11.1	1000	20.83
4	25.6	1100	36.11
6	40.6	1200	51.38
8	53.9	1300	61.11
10	72.3	1400	70.83

Table 13: Antibacterial Activity of Optimized Dapsone Transferosomal Gel against *Staphylococcus aureus* and *Escherichia coli*.

Microorganism	Sample	Concentration (µg/well)	Zone of Inhibition (mm)
Staphylococcus aureus	Optimized dapsone transferosomal gel	100	20.5±0.3
	Reference marketed gel (Acnedep® gel)	100	18.7±0.4
	Normal saline (negative control)	100	No zone
Escherichia coli	Optimized dapsone transferosomal gel	100	18.2±0.4
	Reference marketed gel (Acnedep® gel)	100	15.8±0.5
	Normal saline (negative control)	100	16.3 ± 0.5 mm

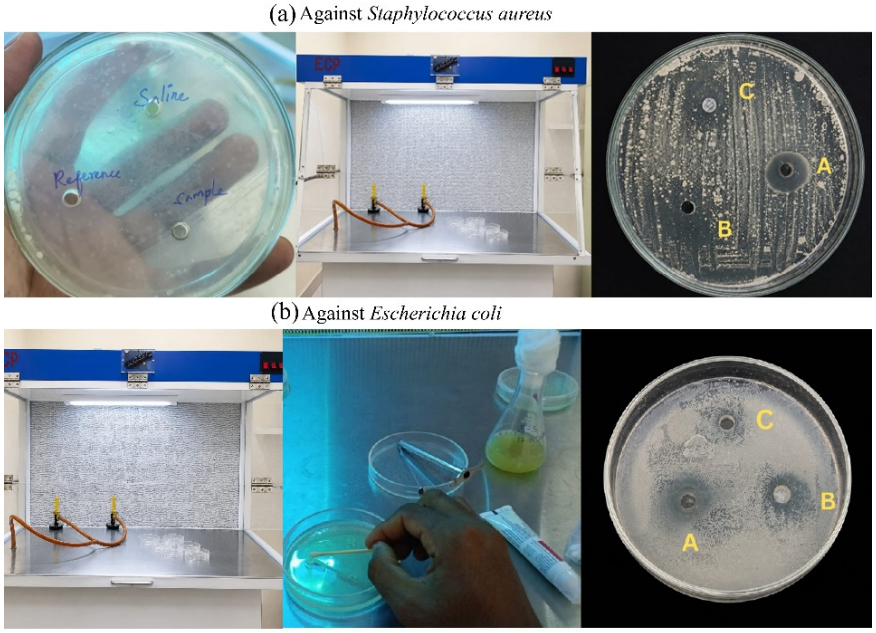


Figure 15: Antibacterial Activity of Optimized Dapsone Transferosomal Gel against *Staphylococcus aureus* and *Escherichia coli*.

translationally relevant alternative to topical dapsone treatments, which is mechanistically well founded.

CONCLUSION

An optimized dapsone-loaded transferosomal gel was successfully developed and systematically optimized by a Quality-by-Design (QbD) approach by using a three-factor, three-level Box-Behnken Design (33 BBD). The dominant factors identified for vesicle size, EE and drug release were lipid concentration and edge-activator concentration which was used for the rational selection of the optimized formulation of lipid concentration 100 mg, edge-activator concentration 25.20 mg and the ratio of chloroform: methanol 1.48 with high overall desirability (0.885). The optimized formulation showed the nanosized vesicles with negative charge (-30.6 mV) and high entrapment efficiency (84.30%) along with drug-excipient compatibility, and good physicochemical gel property. Sustained, non-Fickian drug release was observed in *in vitro* release studies (88.10% at 12 hr) with potent antioxidant activity and improved antibacterial activity against both Gram-positive and gram-negative bacteria as compared to marketed reference product. The optimized transferosomal gel also showed good physical stability with regard to the appearance, drug content, and entrapment efficiency during 45 days of storage under both refrigerated and room temperature. Better storage stability at refrigeration temperature showed lower leakage of the drug and better long-term storage stability of the formulation. Overall, the finding Results indicated that optimized transferosomes based on Box-Behnken design could be promising nanocarrier systems for broad spectrum topical delivery of dapsone for the management of acne vulgaris.

ACKNOWLEDGEMENT

The authors thank the Department of Pharmaceutics, The Erode College of Pharmacy, for providing the laboratory facilities used in this study.

ABBREVIATIONS

AIC: Akaike Information Criterion; **BBD:** Box-Behnken Design; **CDR:** Cumulative Drug Release; **CQA:** Critical Quality Attribute; **DLS:** Dynamic Light Scattering; **DPPH:** 2,2-Diphenyl-1-picrylhydrazyl; **DR:** Drug Release; **EA:** Edge Activator; **EE:** Entrapment Efficiency; **ELS:** Electrophoretic Light Scattering; **FTIR:** Fourier Transform Infrared Spectroscopy; **MSC:** Model Selection Criterion; **PDI:** Polydispersity Index; **PBS:** Phosphate-Buffered Saline; **QbD:** Quality by Design; **ROS:** Reactive Oxygen Species; **SEM:** Scanning Electron Microscopy; **Vs:** Vesicle Size; **ZP:** Zeta Potential.

CONFLICT OF INTEREST

The authors declare that there is no conflict of interest.

FUNDING

The authors declare that this research received no external funding.

ADDITIONAL STATEMENT

The authors confirm that no paper mill was used in the preparation of this manuscript and that all data were generated and analyzed by the authors.

ETHICS APPROVAL AND CONSENT

This article does not contain any studies involving human participants or animals performed by any of the authors. Consent to Participate: Not applicable. Consent for Publication: Not applicable. Clinical Trial Registration: Not applicable.

DATA AVAILABILITY STATEMENT

The datasets generated and/or analyzed during the current study are available from the corresponding author on reasonable request.

AUTHORS CONTRIBUTION

V.A.N.: Conceptualization, Methodology, Writing - Original Draft. **V.S.:** Investigation, Formal Analysis, Writing - Review and Editing. **P.P.:** Data Curation, Validation. S.K.: Supervision, Project Administration. All authors approved the final manuscript.

REFERENCES

1. Dawson AL, Dellavalle RP, Elston DM. Infectious skin diseases: a review and needs assessment. Dermatol Clin. 2012;30(1):141-51. doi:10.1016/j.det.2011.08.003
2. Yakupu A, Aimaier R, Yuan B, Chen B, Cheng J, Zhao Y, *et al.* The burden of skin and subcutaneous diseases: findings from the global burden of disease study 2019. Front Public Health. 2023;11:1145513. doi:10.3389/fpubh.2023.1145513
3. Baskaran N, Arunima A, Shah S, Narang T, Kumaran MS. Psychological morbidity in chronic dermatological disorders: a review. Indian Dermatol Online J. 2025;16(3):381-8. doi:10.4103/idoj.idoj_458_24
4. Kosmoski G, Miller D, Coret C, Atillasoy E. A topical combination regimen of benzoyl peroxide and retinol moisturizer for mild to moderate acne. J Drugs Dermatol. 2022;21(12):1340-6. doi:10.36849/JDD.6845
5. Jaiswal S, Jawade S, Madke B, Gupta S. Recent trends in the management of acne vulgaris: a review focusing on clinical studies in the last decade. Cureus. 2024;16(3):e56596. doi:10.7759/cureus.56596
6. Opatha SAT, Titapiwatanakun V, Chutoprapat R. Transfersomes: a promising nanoencapsulation technique for transdermal drug delivery. Pharmaceutics. 2020;12(9):855. doi:10.3390/pharmaceutics12090855
7. Matharoo N, Mohd H, Michniak-Kohn B. Transferosomes as a transdermal drug delivery system: dermal kinetics and recent developments. Wiley Interdiscip Rev Nanomed Nanobiotechnol. 2024;16(1):e1918. doi:10.1002/wnan.1918
8. Fernández-García R, Lalatsa A, Statts L, Bolás-Fernández F, Ballesteros MP, Serrano DR. Transferosomes as nanocarriers for drugs across the skin: quality by design from lab to industrial scale. Int J Pharm. 2020;573:118817. doi:10.1016/j.ijpharm.2019.118817
9. Alsuwaidan SN, Qadoumi TA. Safety and effectiveness of topical dapsone in acne treatment: a review. J Family Med Prim Care. 2026;15(1):33-8. doi:10.4103/jfmpc.jfmpc_256_25
10. Nickles MA, Lake E. Topical dapsone in the treatment of acne: a systematic review. Int J Dermatol. 2022;61(11):1412-21. doi:10.1111/ijd.16074
11. Wozel G, Blasum C. Dapsone in dermatology and beyond. Arch Dermatol Res. 2014;306(2):103-24. doi:10.1007/s00403-013-1409-7
12. Phatale V, Vaiphei KK, Jha S, Patil D, Agrawal M, Alexander A. Overcoming skin barriers through advanced transdermal drug delivery approaches. J Control Release. 2022;351:361-80. doi:10.1016/j.jconrel.2022.09.025
13. Sim YS, Wong LC, Yeoh SC, Almashhadani A, Alrimawi BH, Goh CF. Skin penetration enhancers: mechanistic understanding and their selection for formulation and design. Drug Deliv Transl Res. 2025;15(11):3864-98. doi:10.1007/s13346-025-01809-9
14. Medhi J, Thalluri C, Vasam M, Bukke SPN. The future of vesicular drug delivery: transferosomes in therapeutic advancement — applications, innovations and challenges. Biomed Eng Online. 2026;25(1):1. doi:10.1186/s12938-025-01490-6
15. Shafi S, Swami S, Waghmare P, Gadhave A, Damane M. Transferosomes: a next-generation ultra-deformable vesicular system — structure, mechanism, and future prospects. Asian J Pharm Res Dev. 2025;13(6):109-18. doi:10.22270/ajprd.v13i6.1661
16. Deng P, Masoud RE, Alamoudi WM, Zakaria MY. Employment of PEGylated ultra-deformable transferosomes for transdermal delivery of tapentadol with boosted bioavailability and analgesic activity. Int J Pharm. 2022;628:122274. doi:10.1016/j.ijpharm.2022.122274
17. Pahwa R, Pal S, Saroha K, Waliyan P, Kumar M. Transferosomes: unique vesicular carriers for effective transdermal delivery. J Appl Pharm Sci. 2021;11(5):1-8. doi:10.7324/JAPS.2021.110501
18. Sapkota R, Dash AK. Liposomes and transferosomes: a breakthrough in topical and transdermal delivery. Ther Deliv. 2021;12(2):145-58. doi:10.4155/tde-2020-0122
19. De A, Dey S, Pradhan PK, Chaudhari F, Patel M. Estimation of dapsone in bulk and dosage form by UV spectroscopic method. Indo Am J Pharm Res. 2014;4(1):312-9.
20. Nangare G, Tegeli V, Ingle S, Matole V, Birajdar A, Adlinge S. UV spectrophotometric analysis and validation of dapsone in semisolid dosage form. Res J Pharm Technol. 2021;14(9):5007-9. doi:10.52711/0974-360X.2021.00872
21. Uwaezuoke O, Du Toit LC, Kumar P, Ally N, Choonara YE. Linoleic acid-based transferosomes for topical ocular delivery of cyclosporine A. Pharmaceutics. 2022;14(8):1695. doi:10.3390/pharmaceutics14081695
22. Chaves LL, Vieira AC, Ferreira D, Sarmento B, Reis S. Rational and precise development of amorphous polymeric systems with dapsone by response surface methodology. Int J Biol Macromol. 2015;81:662-71. doi:10.1016/j.ijbiomac.2015.08.009
23. Hayashi K, Shimanouchi T, Kato K, Miyazaki T, Nakamura A, Umakoshi H. Span 80 vesicles have a more fluid, flexible and "wet" surface than phospholipid liposomes. Colloids Surf B Biointerfaces. 2011;87(1):28-35. doi:10.1016/j.colsurfb.2011.04.029
24. Tian H, Lu Z, Li D, Hu J. Preparation and characterization of citral-loaded solid lipid nanoparticles. Food Chem. 2018;248:78-85. doi:10.1016/j.foodchem.2017.11.091
25. Estupiñan OR, Garcia-Manrique P, Blanco-Lopez MDC, Matos M, Gutiérrez G. Vitamin D3 loaded niosomes and transfersomes produced by ethanol injection method: identification of the critical preparation step for size control. Foods. 2020;9(10):1367. doi:10.3390/foods9101367
26. Rajan R, Jose S, Mukund VP, Vasudevan DT. Transferosomes — a vesicular transdermal delivery system for enhanced drug permeation. J Adv Pharm Technol Res. 2011;2(3):138-43. doi:10.4103/2231-4040.85524
27. Tamilarasan N, Yasmin Begum M, Anitha P, Umme H, Cheng W, Mohan S, *et al.* Box-Behnken design: optimization of proanthocyanidin-loaded transferosomes as an effective therapeutic approach for osteoarthritis. Nanomaterials. 2022;12(17):2954. doi:10.3390/nano12172954
28. Chauhan P, Tyagi BK. Herbal novel drug delivery systems and transfersomes. J Drug Deliv Ther. 2018;8(3):162-8. doi:10.22270/jddt.v8i3.1772
29. Fang JY, Hwang TL, Huang YL, Fang CL. Enhancement of the transdermal delivery of catechins by liposomes incorporating anionic surfactants and ethanol. Int J Pharm. 2006;310(1-2):131-8. doi:10.1016/j.ijpharm.2005.12.004
30. Ahad A, Al-Saleh AA, Al-Mohizea AM, Al-Jenoobi FI, Raish M, Yassin AEB, *et al.* Formulation and characterization of novel soft nanovesicles for enhanced transdermal delivery of eprosartan mesylate. Saudi Pharm J. 2017;25(7):1040-6. doi:10.1016/j.jsps.2017.01.006

31. Adnan M, Ahmad L, Dar MJ, Jamshaid H, Noman M, Faheem M. Formulation, optimization, and evaluation of transferosomes co-loaded with methotrexate and sorafenib for anti-arthritic activity. Pharmaceutics. 2025;17(9):1196. doi:10.3390/pharmaceutics17091196.

Cite this article: Narayanaa VA, Sureshkumar V, Palanisamy P, Kumar S. Development and Optimization of Dapsone-Loaded Transferosomal Gel for Enhanced Topical Delivery in *Acne vulgaris* Using a Box-Behnken Design. Indian J of Pharmaceutical Education and Research. 2027;61:10.5530/ijper.20270039.